Amino Acids (2012) 42:1269–1275
DOI 10.1007/s00726-010-0819-5

ORIGINAL ARTICLE

Evidence for a slow and oxygen-insensitive intra-molecular long range electron transfer from tyrosine residues to the semi-oxidized tryptophan 214 in human serum albumin: its inhibition by bound copper (II)

Larry K. Patterson · Jean-Claude Mazière · David M. Bartels · Gordon L. Hug · René Santus · Patrice Morlière

Received: 23 September 2010 / Accepted: 22 November 2010 / Published online: 5 December 2010

Abstract A slow, long range electron transfer (SLRET) in human serum albumin (HSA) is observed from an intact tyrosine (Tyr) residue to the neutral tryptophan (Trp) radical (Trp·) generated in pulse radiolysis. This radical is formed, at neutral pH, through oxidation with $Br_2^{\cdot-}$ radical anions of the single Trp 214 present. The SLRET rate constant of $\sim 0.2\ s^{-1}$ determined is independent of HSA concentration and radiation dose, consistent with an intra-molecular process. This is the slowest rate constant so far reported for an intra-molecular LRET. In sharp contrast with the LRET reported for other proteins, the SLRET observed here is insensitive to oxygen, suggesting that the oxidized Trp is inaccessible to—or do not react with radiolytically generated $O_2^{\cdot-}$. In N_2O-saturated solutions, the SLRET is inhibited by Cu^{2+} ions bound to the His 3 residue of the N-terminal group of HSA but it is partially restored in O_2-saturated solutions.

Keywords Protein oxidation · Redox metal ions · Pulse radiolysis · Superoxide radical anion · Transient absorbance spectra · Kinetics

Abbreviations

HSA	Human serum albumin
LRET	Long range electron transfer
SLRET	Slow long range electron transfer

Introduction

Protein oxidation in vivo is inherent to aerobic life. Activated oxygen species and other free radicals—produced as by-products of cellular metabolism and generated through the normal function of phagocytic cells or through photochemical reactions—can modify amino acid residues of proteins. Subsequently, loss of protein structure and function can occur through denaturation, fragmentation and/or aggregation (Grune et al. 1998). It has been established that, in aqueous solutions, most amino acid residues are susceptible to oxidation by OH·, the strongest known oxidant in vivo (Davies 1987). Milder oxidants such as lipid peroxyl radicals produced in the peroxidative chain reactions of lipids react more selectively with Trp, Tyr, Glu and Cys while a weak oxidant, such as, $O_2^{\cdot-}$, can sluggishly

L. K. Patterson · D. M. Bartels · G. L. Hug
Radiation Laboratory, University of Notre Dame, Notre Dame, IN 46556, USA

L. K. Patterson · J.-C. Mazière · R. Santus · P. Morlière
Laboratoire de Biochimie, CHU Amiens, place Victor Pauchet, 80054 Amiens, France

J.-C. Mazière · P. Morlière
Faculté de Médecine et de Pharmacie, EA4292, Université de Picardie Jules Verne, 1 rue des Louvels, 80036 Amiens, France

J.-C. Mazière · P. Morlière
INSERM, ERI12, 1 rue des Louvels, 80036 Amiens, France

P. Morlière (✉)
Laboratoire de Biochimie, INSERM ERI 12, CHU Amiens, Hôpital Nord, place Victor Pauchet, 80054 Amiens Cedex 01, France
e-mail: morliere.patrice@chu-amiens.fr

R. Santus
Département RDDM, Muséum National d'Histoire Naturelle, 43 rue Cuvier, 75231 Paris, France

react with Cys residues (Davies 1987; Neta et al. 1990). In the case of Trp or Tyr residues, primary transient species, such as the neutral Trp· and TyrO· radicals, can be produced in pulse radiolysis with the strongly oxidizing OH· radical or with more selective oxidants such as $Br_2^{\cdot-}$, $(SCN)_2^{\cdot-}$ or N_3· (Adams 1973). In some instances, oxidized residues and especially the neutral Trp· radical can be reduced in proteins by antioxidants, such as the ascorbate anion (Jovanovic and Simic 1985), or by inter- and/or intramolecular long range electron transfer (LRET) from Tyr residues to the neutral Trp· radical. This latter behaviour was originally reported by Butler and co-workers (Butler et al. 1982). Pulse radiolysis studies have demonstrated that LRET is modulated in proteins by factors such as proximity, microenvironment and conformation (Butler et al. 1982; Houée-Levin and Sicard-Roselli 2001; Lee et al. 1992). Furthermore, in addition to ascorbate anions, other electron donors such as the $O_2^{\cdot-}/O_2$ redox couple can eliminate LRET (Santus et al. 2000). In these previous studies, the rather short time scales (up to tens of ms) of observation for which most pulse radiolysis instruments have been optimally designed as well as the presence of several Trp residues in the proteins studied, have presented strong limitations to a full understanding of the factors governing LRET.

In the present study, the possible occurrence of LRET processes extending over tens of seconds has been investigated using a rapid scan spectrophotometer which provides spectral and kinetics measurements of high resolution over the minute time scale. To this end, neutral Trp· and TyrO· radicals have been produced by reaction of $Br_2^{\cdot-}$ radical anions with native human serum albumin (HSA) (Filipe et al. 2002a). This protein has been chosen for several reasons. First, it contains a single Trp residue (Trp 214). Secondly, it is a circulating protein thus susceptible to undergo oxidation by radical species such as $O_2^{\cdot-}$ and OH· radicals, produced by the oxidative burst of phagocytic cells. Furthermore, as a carrier of numerous photosensitizing drugs, HSA can also be the target of in situ photosensitized type I radical reactions occurring in sun-exposed skin areas. It has been shown, e.g., that photosensitization by non-steroidal anti-inflammatory drugs of the arylpropionic family bound to HSA produces neutral Trp· radicals (de Vries et al. 1997). Further, about 95% of the total copper (1 μg mL^{-1}) circulating in human plasma, in vivo, is bound to ceruloplasmin (Sengupta et al. 2001), while the remaining and tissue-exchangeable copper (II) is bound to HSA forming tight 1:1 complexes with the His 3 residue (Kragh-Hansen 1981). Thus, oxidation of HSA under controlled conditions by pulse radiolysis is particularly interesting since it allows one to study the effects on LRET of redox metal ions and oxygen or their combination.

Materials and methods

Chemicals

All chemicals were of analytical grade and were used as received. Fatty acid-free HSA was purchased from Sigma (St Louis, Mo, USA). Phosphate buffer (pH 7) was prepared in pure water obtained from a reverse osmosis system from Ser-A-Pure Co. The water exhibits a resistivity of >18 MΩ cm^{-1} and a total organic content of <10 ppb. Solutions were purged with pure N_2O or O_2.

Pulse radiolysis

Pulse radiolysis measurements were carried out with the Notre Dame Radiation Laboratory 8-MeV linear accelerator, which provides 5 ns pulses of up to 30 Gy. In general, the doses used here were approximately 5–10 Gy. The principles of the detection system used for time scales up to 50 ms have been previously described (Hug et al. 1999; Patterson and Lilie 1974). For longer time scales (up to 1 min), this detection system was replaced by an OLIS rapid scan spectrophotometer equipment with double beam detection making possible, simultaneous kinetic and spectral measurements (Filipe et al. 2007). A Corning O-52 optical filter, removing all wavelengths shorter than 330 nm, was placed in the analyzing light beam preceding the sample cell.

The radical chemical yield (G) is defined as the radical concentration divided by the radiolytic dose and can be expressed as μM Gy^{-1} (or μmol J^{-1} in dilute solution). The radiolytic dose can be determined using the so-called $(SCN)_2^{\cdot-}$ dosimetry consisting in measuring the transient absorbance at 472 nm immediately after the radiolytic pulse. For this dosimetry (10^{-2} mol l^{-1} SCN^- in N_2O-saturated solution), a $G \times \varepsilon$ value for $(SCN)_2^{\cdot-}$ equal to 5.28×10^{-4} m^2 J^{-1} was assumed (Buxton and Stuart 1995) confirmed by Hare and co-workers (Hare et al. 2008). A G value for $Br_2^{\cdot-}$ equal to 0.64 μM Gy^{-1} was used, taking into account the dependence of spur scavenging on Br^- concentration (La Verne and Pimblott 1991). Additionally, production of superoxide radical by oxygen scavenging of H· is included in calculating the G value for $O_2^{\cdot-}$. Numerical integrations, carried out in analyses of rate data, were conducted using Scientist software from Micromath Scientific Software.

Solutions for pulse radiolysis were prepared in 10 mM phosphate buffer (pH 7) and contained 0.1 M Br^-. To conserve costly high purity grade HSA, a microcell (optical path: 1 cm, volume 120 μL and 2 mm i.d. Teflon® tubing) was used for transient recording. As kinetics were seen change with repeated radiation; solution in the cell was completely drained and replaced between the pulses. For

this purpose, an automated two syringe system—one for withdrawing irradiated solution and one for refilling the cell—was employed.

Results and discussion

One-electron oxidation of HSA by $Br_2^{\cdot-}$ radical anions in N_2O-saturated buffer

Pulse radiolysis of a N_2O-saturated buffered aqueous solution containing 0.1 M Br^-, generates $Br_2^{\cdot-}$ radical anions by the sequence of reactions:

$$H_2O \rightarrow e_{aq}, H\cdot, OH\cdot, H_2O_2$$

$$e_{aq} + N_2O \rightarrow OH\cdot + N_2 + OH^- \quad (1)$$

$$OH\cdot + 2Br^- \rightarrow Br_2^{\cdot-} + OH^- \quad (2)$$

The $Br_2^{\cdot-}$ radical anion is produced with a radiolytic yield of 0.64 μM Gy^{-1}. In the absence of HSA, it decays by second order kinetics with a bimolecular reaction rate constant of $2k_3 = 4.3 \times 10^9$ M^{-1} s^{-1} via the recombination reaction (Filipe et al. 2002b):

$$2Br_2^{\cdot-} \rightarrow 2Br^- + Br_2 \quad (3)$$

The $Br_2^{\cdot-}$ radical is very reactive with native HSA as illustrated by the bimolecular reaction rate constant, $k_4 = 2 \times 10^9$ M^{-1} s^{-1}, previously reported (Filipe et al. 2002a) for the reaction:

$$Br_2^{\cdot-} + HSA \rightarrow \text{products} \quad (4)$$

With the radiolytic doses and HSA concentration used in these experiments, all $Br_2^{\cdot-}$ radicals decay within less than 1 ms by reactions (3) and (4) (data not shown). The high reactivity of HSA with $Br_2^{\cdot-}$ results from multiple targets in this protein which contains a single Trp (Trp 214), a single Cys (Cys 34), 18 Tyr, 16 His and 6 Met as potential reactive residues (Kragh-Hansen 1981). However, there are marked differences in the reactivity of $Br_2^{\cdot-}$ toward individual amino acids. At pH 7, the reactivity of Trp is five times that of Cys, 50 times that of Tyr and about an order of magnitude greater than that of His or Met (Adams 1973). As reported with other proteins (Adams 1973; Butler et al. 1982; Weinstein et al. 1991), the transient absorption spectra of HSA in the near-UV and visible regions shown in Fig. 1 at various times after oxidation by $Br_2^{\cdot-}$ are due to the presence of TyrO· (maximum absorbance at 410 nm) and Trp· (maximum absorbance at ~520 nm). These spectra reflect the reactivity of the Tyr and Trp residues as well as their physical accessibility to $Br_2^{\cdot-}$ attack. They also suggest the occurrence of sequential reactions. Binding of Cu^{2+} to HSA does not produce major change in the initial transient spectral shape. However, the

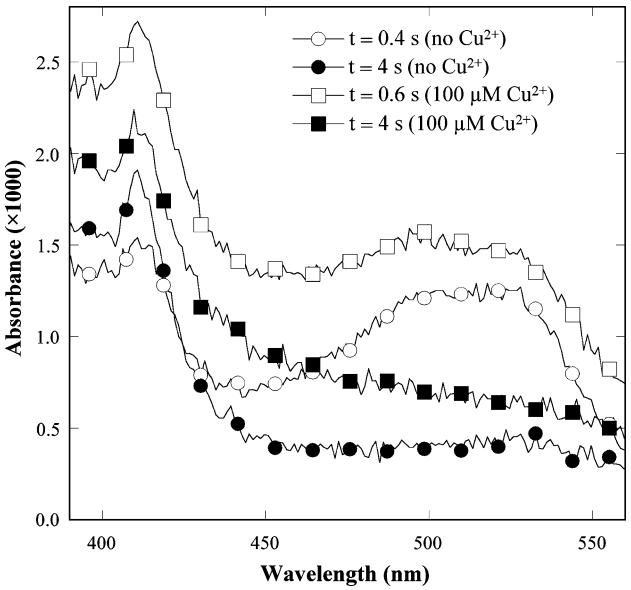

Fig. 1 Transient absorption spectra recorded at various times after pulse radiolysis of N_2O-saturated solutions of 10 mM phosphate buffer (pH 7) containing 0.1 M Br^- and 100 μM HSA in the presence and the absence of 100 μM Cu^{2+}. Dose was 5.4 Gy. Temperature: 20°C

decrease of the 520 nm transient is not accompanied by the increase in the 410 nm transient observed in the absence of Cu^{2+}, over a 4 s period. As a result, a general decrease in both the 410 nm and 520 nm transients occurs (Fig. 1).

Transient kinetics in Fig. 2a demonstrate that in HSA solutions, a slow growth of the 410 nm transient is observed over 4 s after a fast initial growth. The delayed growth of the 410 nm transient parallels a decrease in the Trp transient absorbance at 520 nm (Fig. 2b). As observed with other proteins (Butler et al. 1982; Santus et al. 2000; Weinstein et al. 1991), the secondary growth of the TyrO· can be attributed to LRET from an intact Tyr residue to the oxidized Trp 214:

$$Tyr + Trp\cdot \rightarrow TyrO\cdot + Trp \quad (5)$$

The kinetic data in Fig. 2a, b thus corroborate the transient absorbance changes shown in Fig. 1. To our knowledge, this is the slowest LRET so far reported in native proteins. By contrast, a LRET from Tyr to the oxidized Trp residue has been observed in the millisecond time scale with denatured HSA solutions (Filipe et al. 2002a). The absence of literature data for very slow LRET (SLRET) in HSA is most likely due to the experimental limitations since time scales of kinetic measurements have been limited to 50 ms at most in preceding reports (Butler et al. 1982; Filipe et al. 2002a; Houée-Levin and Sicard-Roselli 2001; Weinstein et al. 1991). It should be noted that Stubbe and co-workers have observed with stopped-flow experiments an intermolecular SLRET occurring with a

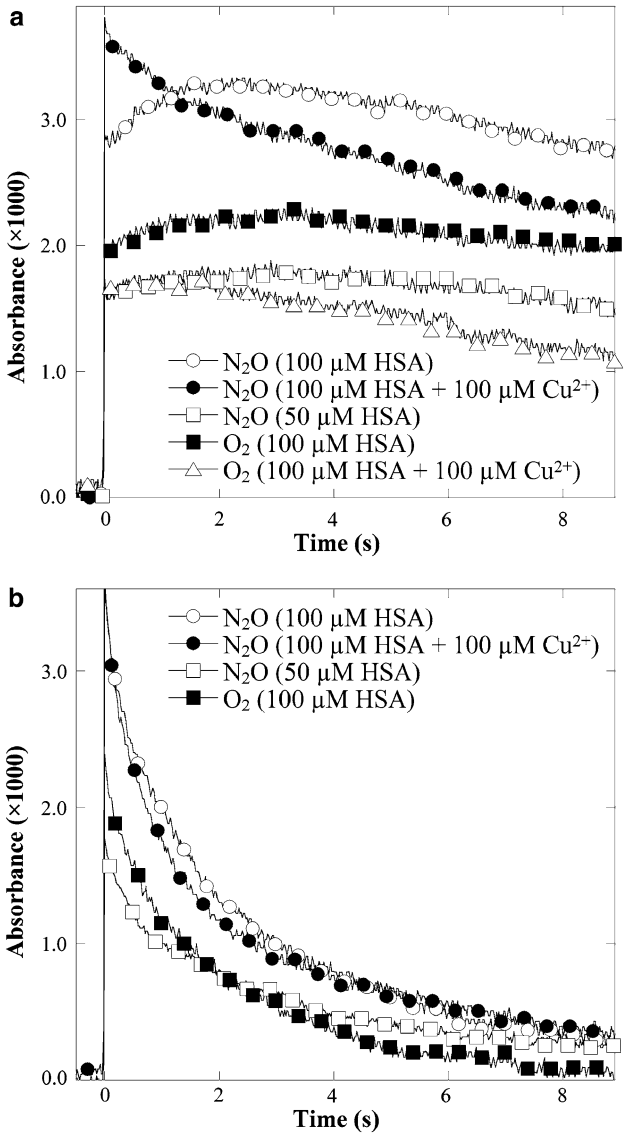

Fig. 2 Time evolution of the transient absorbance measured at **a** 410 nm (maximum absorbance of TyrO·) or **b** 520 nm (maximum absorbance of Trp·) in N_2O- or O_2-saturated solutions of HSA in 10 mM phosphate buffer (pH 7) under the various conditions of concentration indicated in the figure. Dose was 2.9 Gy with 50 μM HSA and 5.4 Gy with 100 μM HSA. Temperature: 20°C

rate constant of 0.04 s between sub-units of mutant forms of the *E. coli* ribonucleotide reductase (Minnihan et al. 2009).

The analysis of the present data and those we have previously reported for denatured HSA suggests that, among the 18 Tyr residues of HSA, several of them—each residing at a different location in the peptide chain—are susceptible to inter- or intra-molecular LRET. Transfer can occur with different probabilities depending upon the degree of accessibility of the Tyr residues to the single semi-oxidized Trp 214. Similar conformational effects have been already reported on much shorter time scales with lysozyme (Santus et al. 2000; Weinstein et al. 1991).

It is generally agreed (Weinstein et al. 1991) that the molar absorbance of aromatic amino acid radicals remains essentially unchanged, whether the amino acid is unbound or is incorporated into a protein. Hence, the radiolytic yield of these radicals can be determined using a molar absorbance of 2,700 M^{-1} cm^{-1} at 410 nm for the TyrO· radical (Weinstein et al. 1991) and 1,750 M^{-1} cm^{-1} at 520 nm for the Trp· radical (Redpath et al. 1975). The contribution of the Trp· transient at 410 nm is only 300 M^{-1} cm^{-1}. Table 1 presents the initial G values of the Trp· and TyrO· radicals (G_i(Trp·) and G_i (TyrO·) after the radiolytic pulse (commencement of the SLRET) as well as G_s(Trp·) and G_s (TyrO·) after the plateau in the TyrO· radical spectrum has been reached, ~3 s following the pulse, as estimated from Fig. 2a, b. The sum of the initial yields, G_i(Trp·) + G_i(TyrO·), resulting from $Br_2^{\cdot-}$ attack is ~25% lower than the initial $G(Br_2^{\cdot-})$ value. The rate equation used, which takes into account the competitive reactions (3) and (4), is:

$$-\mathrm{d}\left[Br_2^{\cdot-}\right]/\mathrm{dt} = 2k_3\left[Br_2^{\cdot-}\right]^2 + k_4\left[Br_2^{\cdot-}\right][\mathrm{HSA}] \qquad (6)$$

The initial $[Br_2^{\cdot-}]$ and the time-dependent [Trp·] reflecting the kinetics of the HSA oxidation are measureable whereas [HSA] which is present in large excess compared to $[Br_2^{\cdot-}]$ can be considered to be constant. As a result, the radiolytic yield of initial HSA oxidation by $Br_2^{\cdot-}$ can be obtained after integration of Eq. (6). The calculation shows that at the dose used, ~5% of the initial $Br_2^{\cdot-}$ radicals do not react with HSA. It can be concluded that ~20% of $Br_2^{\cdot-}$ reacts with residues other than Tyr and Trp. Three-dimensional structure data suggest that the single Cys-34 residue is theoretically the most likely candidate but that this residue is partially protected from the surrounding solvent (He and Carter 1992). As a consequence, oxidation of some His and Met cannot be excluded.

Table 1 Radiolytic yield (G in μM Gy^{-1}) of the TyrO· and Trp· radicals formed by reaction of $Br_2^{\cdot-}$ with HSA at pH 7 before (G_i) and at the plateau (G_s) of the slow long range electron transfer (t = 3 s) in N_2O-saturated 10 mM phosphate buffer (see text)

Radical	G_i	G_s
Trp·	0.365	0.105
TyrO·	0.155	0.22

All the solutions contained 100 μM HSA and 0.1 M KBr. Temperature was 20°C. Radical concentrations were determined at 520 nm (Trp·) and 410 nm (TyrO·) using molar absorbance given in the text. The contribution of the transient absorbance of the Trp· radical at 410 nm was taken into account to calculate G(TyrO·). G values are means of two measurements. Uncertainties in G values are <5%

At the maximal absorbance of TyrO· radical reached after completion of the SLRET (Fig. 2a), $G_s(\text{TyrO}\cdot) = 0.22\ \mu\text{M Gy}^{-1}$ leading to an apparent SLRET yield of only ~20%. At the same time, Table 1 shows that almost 75% of the Trp· radicals have disappeared on the same time scale (see also Fig. 2b). It may be hypothesized that the TyrO· radical is consumed during the SLRET by formation of dityrosine (Francis et al. 1993) by an intermolecular bimolecular recombination reaction:

$$2\text{TyrO}\cdot \rightarrow \text{products} \quad (7)$$

This is suggested by the effect of the HSA concentration on the consumption of TyrO· as reflected in the 410 nm decay kinetics (Fig. 2a). The decay of the Trp· transient absorbance does not follow a simple first order rate law as should be expected from the repair reaction (5) (calculation not shown). Instead, in addition to an intermolecular bimolecular Trp· recombination reaction, the complex kinetics suggest that other reaction paths for the decay of Trp· radicals cannot be excluded:

$$\text{Trp}\cdot + \text{Trp}\cdot\ (\text{or X}) \rightarrow \text{products} \quad (8)$$

where X represents other radical species formed by reaction of $Br_2^{\cdot-}$ radicals with HSA as shown above. The time-dependent [Trp·] can be precisely known by application of a 9th-order polynomial fit to the Trp· transient absorbance decay at 520 nm (calculation not shown). The fast and complex Trp· decay shown in Fig. 2a, may well contribute to the complex kinetics observed at 410 nm and which was previously attributed to a "fast" LRET observed when using the conventional pulse radiolysis detection system (Filipe et al. 2002a). Taking into account reactions (5, 7, 8) the rate equation for the time dependence of the 410 nm transient can be written as:

$$-\text{d}[\text{TyrO}\cdot]/\text{dt} = -k_5[\text{Trp}\cdot] + 2k_7[\text{TyrO}\cdot]^2 \quad (9)$$

where [Trp·] calculated directly from observation above and time "t" are the sole independent variables. This kinetic scheme is supported by the excellent time-dependent fit of the [TyrO·] leading to first order rate constants k_5 of 0.20 s^{-1} and 0.17 s^{-1} for the SLRET in N_2O-saturated solutions with 100 or 50 μM HSA, respectively (Fig. 3). These essentially concentration- and dose-independent growth rate constants (see legend of Fig. 3) strongly underline the intramolecular nature of the SLRET. Parenthetically, the fit of 410 nm decay produces bimolecular reaction rate constants of $2k_7 = 4.5 \times 10^4\ \text{M}^{-1}\ \text{s}^{-1}$ and $2k_7 = 6.8 \times 10^4\ \text{M}^{-1}\ \text{s}^{-1}$ with 100 and 50 μM HSA, respectively. The reasonable agreement between these two values obtained under different radiolytic dose conditions supports dityrosine formation as a main pathway for the TyrO· decay.

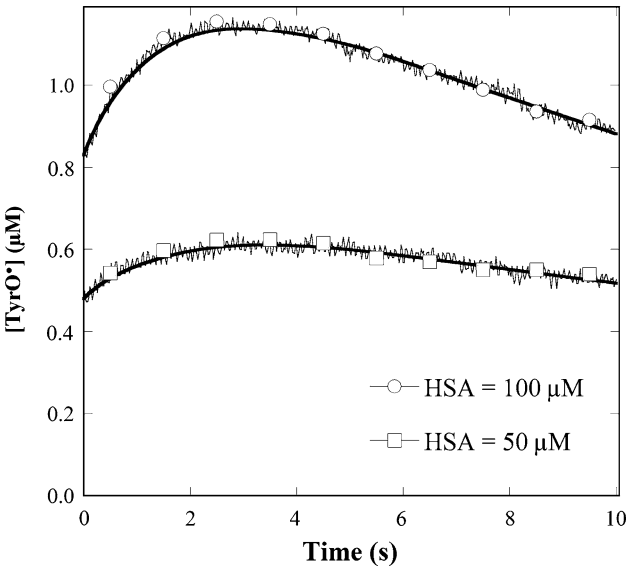

Fig. 3 Fit of the time-dependent change in the TyrO· concentration according to rate Eq. (9) (*solid line*) after pulse radiolysis of 100 and 50 μM HSA in N_2O-saturated buffered (pH7) solutions containing 0.1 M Br^-. Dose was 2.9 Gy with 50 μM HSA and 5.4 Gy with 100 μM HSA. The TyrO· radical concentration was calculated using Fig. 2a data. The molar absorbance of TyrO· and Trp· radicals at 410 nm is given in the text

Insensitivity of the SLRET to $O_2^{\cdot-}$ radical anions

Pulse radiolysis of an O_2-saturated solution containing 0.1 M Br^- produces $O_2^{\cdot-}$ at yield $G = 0.34\ \mu\text{M Gy}^{-1}$ following reactions:

$$e_{aq} + O_2 \rightarrow O_2^{\cdot-} \quad (10)$$

$$\text{H}\cdot + O_2 \rightarrow O_2^{\cdot-} + \text{H}^+ \quad (11)$$

and the radiolytic yield of $Br_2^{\cdot-}$ radical formed according to the Eq. (2) is reduced to 0.32 $\mu\text{M Gy}^{-1}$. This is reflected in the smaller transient absorbances (Fig. 2a, b) and yields (Table 2) of Trp· and TyrO· radicals as compared to those measured in N_2O-saturated solutions (Table 1). As opposed to other proteins such as lysozyme where most Trp· radicals readily react with $O_2^{\cdot-}$ radicals (Santus et al. 2000), the Trp· radical decay is essentially insensitive to the presence of oxygen. Figure 2a demonstrates clearly that the SLRET is still observed and occurs at a rate similar to that in N_2O-saturated solutions. Two conclusions may be drawn from these data. First, once formed, Trp· is inaccessible to—or unreactive with—the superoxide radical anion despite the observation that, Trp 214 in its native micro-environment reacts readily with the negatively charged $Br_2^{\cdot-}$ radical. Secondly, O_2 does not act as an electron scavenger in the LRET process from a Tyr residue to Trp 214.

Table 2 Initial radiolytic yield (G in μM Gy^{-1}) of the TyrO· and Trp· radicals formed by reaction of $Br_2^{\cdot-}$ with 100 μM HSA at pH 7 under various experimental conditions

Conditions	N_2O, Cu^{2+}	O_2	O_2, Cu^{2+}
G(Trp·)	0.365	0.22	0.185
G(TyrO·)	0.24	0.09	0.09

Radical concentrations were determined at 520 nm (Trp·) and 410 nm (TyrO·) as in Table 1

N_2O, Cu^{2+} N_2O-saturated 10 mM phosphate buffer containing 100 μM $CuSO_4$

O_2 O_2-saturated 10 mM phosphate buffer

O_2, Cu^{2+} O_2-saturated 10 mM phosphate buffer containing 100 μM $CuSO_4$

Effect of bound Cu^{2+} ions on the SLRET

The Cu^{2+} ion strongly binds to His 3 at the N-terminal end of HSA, a flexible region of the molecule comprising the first three residues. This behaviour has been deduced from the atomic structure at 0.28 nm resolution (He and Carter 1992). The binding of one Cu^{2+}/HSA induces a minimal 7% quenching of the Trp 214 fluorescence, suggesting that the single Trp residue is not in the vicinity of bound copper (Filipe et al. 2004). The Cu^{2+} binding, however, produces dramatic effects on the SLRET. Figure 2a demonstrates that SLRET is totally inhibited by bound Cu^{2+} in N_2O saturated solutions whereas the initial G(TyrO·) radical yield is increased by about 20% (Table 2; Fig. 2a). The yield of the G(Trp·) radical remains unaffected (Fig. 2b). It is also observed that the reaction rate constant for the intermolecular recombination reaction of the TyrO· ($2k_7 = 2.8 \times 10^4$ M^{-1} s^{-1}) is significantly increased in the presence of Cu^{2+} ions as suggested by transient decays shown in Fig. 2a. The Trp· decay is also significantly modified with the appearance of a very long lived component. The kinetic data illustrate the general decrease in the transient absorbance in the time interval 0–4 s shown in Fig. 1.

An additional striking effect of Cu^{2+} ions in this system is the partial restoration of the SLRET in O_2-saturated solutions (Fig. 2a). When combined, these results suggest that the freely moving N-terminal tail of HSA can interfere with the SLRET by bringing redox Cu^{2+} ions into the vicinity of the Tyr residue(s) involved in the electron transfer. Moreover, when bound to the basic His 3 residue, a positively charged Cu^{2+} ion is a better oxidant than a free Cu^{2+} due to the electronic attraction between the Cu^{2+}-His complex and negatively charged species (Yamashoji et al. 1977). As a result, it may catalyze the one-electron oxidation of an otherwise relatively unreactive Tyr residue by the $Br_2^{\cdot-}$ radical. This may provide an explanation for the increased TyrO· yield in the presence of bound copper and the partial SLRET recovery in the presence of $O_2^{\cdot-}$ radicals which can reduce HSA bound copper (II) at a rate constant of 6.1×10^6 M^{-1} s^{-1} (Filipe et al. 2004). This reaction could compete with that between $Br_2^{\cdot-}$ and HSA. A consideration of the three-dimensional picture of HSA (PDB accession number 1UOR at http://www.rcsb.org) suggests that only residues Tyr 30 and Tyr 353 are close enough to both Trp 214 and His 3 to be prone to such redox interferences in the SLRET process.

Conclusions

The application of a dual beam pulse radiolysis detection system provides the means for measurement at high precision of radical behaviour which occurs in long time and is—due to micro-environmental and structural considerations—inherent to biological systems. Application of this system reveals electron transfer processes occurring on the time scale of seconds, not previously reported. Of particular interest here are the roles played by bound Cu^{+2} and the presence of O_2 in altering the kinetics of radical production and subsequent SLRET in HSA.

The inhibition of SLRET by bound Cu^{2+} ions after one-electron oxidation of HSA by $Br_2^{\cdot-}$ with a parallel increase in the initial TyrO· yield is of general interest for the understanding of LRET processes in proteins. It suggests that a redox metal ion such as Cu^{2+} bound to a single residue may act as an electron shuttle to favour the one-electron oxidation of protein residues by relatively mild oxidants such as $Br_2^{\cdot-}$. Native HSA is a good model for the demonstration of such a process since available crystallographic data show that Cu^{2+} binding to the N-terminal end of the protein does not greatly perturb the gross protein conformation (He and Carter 1992). The transient formation of Cu^{+} species during the course of the LRET is strongly supported by the partial restoration of the SLRET by $O_2^{\cdot-}$ which is known to react with the Cu^{2+}-HSA complex (Filipe et al. 2004). Another factor that may favour the occurrence of a slow LRET may well be a local re-organization of the protein tertiary structure induced over seconds by the modification of the several protein residues during oxidation. This interpretation is supported by the observations presented here with $Br_2^{\cdot-}$ as oxidant. The assessment of the general occurrence and kinetic aspects of delayed redox processes following an initial oxidative stress, as exemplified here, merit further studies with other proteins. Such efforts may reveal very slow mechanisms—not observed to date—or protein degradation at sites well removed from those of initial radical formation. Such mechanisms may well have implications for the overall understanding of radical induced protein degradation in cellular systems.

Acknowledgments This is Document No. NDLR-4892 from the Notre Dame Radiation Laboratory which is supported by the Office of Basic Energy Sciences at the United States Department of Energy.

References

Adams GE (1973) Radiation chemical mechanisms in radiation biology. In: Burton M, Magee JL (eds) Advances in radiation chemistry, vol 3. John Wiley and Sons, New York, pp 146–159

Butler J, Land EJ, Prutz WA, Swallow AJ (1982) Charge transfer between tryptophan and tyrosine in proteins. Biochim Biophys Acta 705:150–162

Buxton GV, Stuart CR (1995) Reevaluation of the thiocyanate dosimeter for pulse radiolysis. J Chem Soc Faraday Trans 91:279–281

Davies KJ (1987) Protein damage and degradation by oxygen radicals. I. General aspects. J Biol Chem 262:9895–9901

de Vries H, Encinas S, Miranda MA, Castell JV, Beijersbergen van Henegouwen GM (1997) Photodegradation and photobinding of tiaprofenic acid: in vitro versus in vivo. Photochem Photobiol 66:432–435

Filipe P, Morlière P, Patterson LK, Hug GL, Mazière J-C, Mazière C, Freitas JP, Fernandes A, Santus R (2002a) Mechanisms of flavonoid repair reactions with amino acid radicals in models of biological systems: a pulse radiolysis study in micelles and human serum albumin. Biochim Biophys Acta 1572:150–162

Filipe P, Morlière P, Patterson LK, Hug GL, Mazière J-C, Mazière C, Freitas JP, Fernandes A, Santus R (2002b) Repair of amino acid radicals of apolipoprotein B100 of low-density lipoproteins by flavonoids. A pulse radiolysis study with quercetin and rutin. Biochemistry 41:11057–11064

Filipe P, Morlière P, Patterson LK, Hug GL, Mazière J-C, Freitas JP, Fernandes A, Santus R (2004) Oxygen-copper (II) interplay in the repair of semi-oxidized urate by quercetin bound to human serum albumin. Free Radic Res 38:295–301

Filipe P, Patterson LK, Bartels DM, Hug GL, Freitas JP, Mazière J-C, Santus R, Morlière P (2007) Albumin-bound quercetin repairs vitamin E oxidized by apolipoprotein radicals in native HDL3 and LDL. Biochemistry 46:14305–14315

Francis GA, Mendez AJ, Bierman EL, Heinecke JW (1993) Oxidative tyrosylation of high density lipoprotein by peroxidase enhances cholesterol removal from cultured fibroblasts and macrophage foam cells. Proc Natl Acad Sci USA 90:6631–6635

Grune T, Blasig IE, Sitte N, Roloff B, Haseloff R, Davies KJA (1998) Peroxynitrite increases the degradation of aconitase and other cellular proteins by proteasome. J Biol Chem 273:10857–10862

Hare PM, Price EA, Bartels DM (2008) Hydrated electron extinction coefficient. J Phys Chem A 112:6800–36802

He XM, Carter DC (1992) Atomic structure and chemistry of human serum albumin. Nature 358:209–215

Houée-Levin C, Sicard-Roselli C (2001) Radiation chemistry of proteins. In: Jonah C, Rao BM (eds) Radiation chemistry: present status and future prospects. Elsevier, New York, pp 553–584

Hug GL, Wang Y, Schoneich C, Jiang PY, Fessenden RW (1999) Multiple time scale in pulse radiolysis: applications to bromide solutions and dipeptides. Radiat Phys Chem 54:559–566

Jovanovic SV, Simic MG (1985) Repair of tryptophan radicals by antioxidants. J Free Radic Biol Med 1:125–129

Kragh-Hansen U (1981) Molecular aspects of ligand binding to serum albumin. Pharmacol Rev 33:17–53

La Verne JA, Pimblott SM (1991) Scavenger and time dependence of radicals and molecular products in the radiolysis of water: examination of experiments and models. J Phys Chem 95:3196–3206

Lee H, Faraggi M, Klapper MH (1992) Long range electron transfer along an alpha-helix. Biochim Biophys Acta 1159:286–294

Minnihan EC, Seyedsayamdost MR, Stubbe J (2009) Use of 3-aminotyrosine to examine the pathway dependence of radical propagation in Escherichia coli ribonucleotide reductase. Biochemistry 48:12125–12132

Neta P, Huie RE, Ross AB (1990) Rate constants for reactions of peroxyl radicals in fluid solutions. J Phys Chem Ref Data 19:413–513

Patterson LK, Lilie JA (1974) Computer-controlled pulse radiolysis system. Int J Radiat Phys Chem 6:129–141

Redpath JL, Santus R, Ovadia J, Grossweiner LI (1975) The oxidation of tryptophan by radical anions. Int J Radiat Biol 27:201–204

Santus R, Patterson LK, Hug GL, Bazin M, Mazière J-C, Morlière P (2000) Interactions of superoxide anion with enzyme radicals: kinetics of reaction with lysosyme tryptophan radicals and corresponding effects on tyrosine electron transfer. Free Radic Res 33:383–391

Sengupta S, Wehbe C, Majors AK, Ketterer ME, DiBello PM, Jacobsen DW (2001) Relative roles of albumin and ceruloplasmin in the formation of homocystine, homocysteine-cysteine-mixed disulfide, and cystine in circulation. J Biol Chem 276:46896–46904

Weinstein M, Alfassi ZB, Defelippis MR, Klapper MH, Faraggi M (1991) Long range electron transfer between tyrosine and tryptophan in hen egg-white lysozyme. Biochim Biophys Acta 1076:173–178

Yamashoji S, Yoshida H, Kajimoto G (1977) Prooxidative effects of Cu^{2+}-amino acid complexes on the autooxidation of linoleic acid. Agric Biol Chem 41:1947–1951